

Effects of Polarization of 1.4 μm Femtosecond Laser Pulses on the Formation and Fragmentation of Naphthalene Molecular Ions Compared at the Same Effective Ionization Intensity

Tomoyuki Yatsunami* and Nobuaki Nakashima

Department of Chemistry, Graduate School of Science, Osaka City University, 3-3-138 Sugimoto, Sumiyoshi, Osaka 558-8585, Japan

Received: July 13, 2005; In Final Form: August 24, 2005

Naphthalene was ionized with 130 fs pulses of different polarizations at 1.4 μm . In contrast to the results of ionization by 0.8 μm pulses, fragmentation was dramatically suppressed and naphthalene molecular ions of up to 3+ were produced. The use of this simple model of ionization and large electron kinetic energy enabled us to study the electron-recollision-induced fragmentation and/or double ionization more precisely. The failure of the theoretical prediction of ion yield for the case of naphthalene prevented us from judging the electron recollision solely by a comparison with theoretical curves. Therefore, the effects of laser polarization on the ratios between differently charged states and between molecular and total ions were compared at the same effective (peak) intensity instead of average intensity. Comparison under the same effective intensity enabled us to identify the effects of ellipticity clearly. Evidence of the electron recollision was found in the doubly charged molecular ion formation but not in the fragmentation. The single-electron recollision event was not sufficient to induce fragmentation because of its low energy transfer efficiency. We concluded that the fragmentation originated in the unstable nature of the highly charged molecular ion itself and in the Coulomb explosion in the case of naphthalene.

Introduction

Ionization is the most fundamental of the processes induced by an intense femtosecond laser.¹ Many experiments and theoretical investigations have been reported in the case of atomic ionization. In the study of molecular ionization, the origin of fragmentation is currently one of the central topics.² Most large molecules show heavy fragmentation with 0.8 μm pulses even at a low-intensity regime ($10^{13} \text{ W cm}^{-2}$). This makes the analysis of experimental results highly complicated and prevents us from comparing the results against theoretical predictions. An intact molecular ion³ and its highly charged state⁴ formation are desirable not only for analytical application but also for fundamental studies. The fragmentation mechanisms that are independent of molecules such as the nonlinear increase of the focal spot area⁵ and the collecting volume effect⁶ were recently investigated. These experimental problems would be avoided, but there exists the fragmentation originating in the nature of the molecules. The importance of radical cations in the postionization fragmentation process has been increasingly recognized, and controversy as to the arguments about fragmentation mechanism is ongoing.^{7,8,9} Evidently, we can use a shorter duration pulse¹⁰ and/or pulses at a suitable wavelength that are off-resonant with the molecular cation radicals to avoid fragmentation.^{11,12} Generally, a longer wavelength is better than a shorter one. When a longer wavelength laser pulse is used for ionization, there are several characteristic advantages as follows: (1) The resonance-induced fragmentation can be suppressed as mentioned above. (2) The tunneling ionization regime is reached at lower intensity. The Keldysh parameter γ defines the border between the multiphoton ionization regime

($\gamma > 1$) and field ionization regime ($\gamma < 1$) of atoms.¹³ For example, γ is 1 at $2.2 \times 10^{13} \text{ W cm}^{-2}$ (1.4 μm) and at $6.8 \times 10^{13} \text{ W cm}^{-2}$ (0.8 μm). (3) We can expect the ejected electron to have a large kinetic energy due to the large ponderomotive force, which is proportional to the square of the laser wavelength. In addition, clear presentations of experimental results have been reported using longer wavelength pulses.¹⁴

The recollision-induced¹⁵ ionization is considered to be the main mechanism of the formation of the doubly charged state in atoms,¹⁶ as well as in few-atom molecules below the sequential-double-ionization regime. As the laser intensity increases, the rate of sequential double ionization exceeds that of nonsequential (recollision-induced) double ionization. As a result, the contribution of recollision-induced double ionization becomes relatively small in the high-intensity region. On the other hand, the electron-recollision-induced fragmentation is expected to occur more efficiently as the laser intensity increases, because the ejected electron gains sufficient kinetic energy in the high-intensity region. However, the literature contains only a few studies on recollision-induced fragmentation and/or highly charged state formation of large molecules such as alcohols,¹⁷ benzene,¹⁸ and C_{60} .¹⁹ We considered that the use of a simple model of ionization (i.e., one without resonance-induced fragmentation) and large electron kinetic energy would enable us to study the electron-recollision-induced fragmentation and/or double ionization more precisely.

In this study, we irradiated naphthalene with a 1.4 μm femtosecond pulse and examined the ellipticity dependencies of the fragmentation and of the formation of highly charge states. The effect of electron recollision was examined by changing the laser polarization from linear to circular. This is because the orbit of a released electron will be altered by the laser

* To whom correspondence should be addressed. E-mail: tomo@sci.osaka-cu.ac.jp.

electronic field and completely miss the ion in the case of circularly polarized light. In these examinations, we should take the effect of laser intensity changes into account. Although we keep the incident laser power (average intensity) constant, the effective (peak) intensity for ionization decreases by changing the polarization from linear to circular. We showed that making the comparison under the same effective intensity enabled us to identify the effect of ellipticity very clearly. On the other hand, the failure of the theoretical prediction of ion yield for the case of naphthalene prevented us from judging the electron recollision solely by a comparison with theoretical curves. Evidence of electron recollision was found in the doubly charged molecular ion formation. However, the fragmentation was independent of the ellipticity. The single-electron recollision event was not sufficient to induce fragmentation because of the low energy transfer efficiency. We concluded that the fragmentation arose due to both the unstable nature of the highly charged molecular ion itself and the Coulomb explosion in the high-intensity region.

Experimental Section

Naphthalene (Nacalai, zone refined) was used without further purification. Xenon was purchased from Japan Air Gases with a stated purity of 99.99%. Xenon was introduced effusively by a leak valve. Naphthalene was heated and introduced effusively through a 1 mm diameter aperture located 40 mm above the laser focus point. The base pressure of the ionization chamber and that of the time-of-flight chamber were below 5×10^{-7} Pa. The sample pressure 20 cm away from the laser focus point was monitored and kept below 5×10^{-5} Pa during the experiments to avoid a space-charge effect. The pressure in the time-of-flight mass chamber was kept to 10 times below that of the ionization chamber by differential pumping.

A 0.5 TW Ti:sapphire laser (Thales laser, alpha 100/XS, <30 fs, 100 Hz, >15 mJ, 800 nm, RMS stability $\sim 1\%$) was used to excite an optical parametric amplifier. In this study, a 100 fs (negatively chirped) pulse of alpha 100/XS was used for pumping the optical parametric amplifier (Quantronix, TOPAS). A 1.4 μm pulse was selected by reflecting it with several dielectric mirrors. The pulse width was measured by a second-order scanning autocorrelator (APE, PulseCheck). The same optical elements, such as the ionization chamber window, focusing lens, and neutral density filter, were placed in front of the autocorrelator to have the same group velocity dispersion. A pulse of 130 fs duration was used for the experiments. A broad-band quarter-wave plate was used to change the laser polarization, and ellipticity was analyzed by using a broad-band polarizing cube beam splitter and photodiode.

A reflection-type time-of-flight mass spectrometer (Toyama, KNTOF-1800, flight length 1.8 m) was used for ion analysis. An aperture of 1 mm diameter was located on the extraction plate to collect the ions that were generated in the most tightly focused point of the laser beam. The output signal from an MCP was averaged by a digital oscilloscope (LeCroy, Wave Runner 6100, 1 GHz) for 1000 shots. The ion yield was obtained by integrating over the appropriate peaks in the time-of-flight spectrum. The resolution ($m/\Delta m$, fwhm) was more than 10^3 at $m/z = 129$.

The direction of laser polarization was orthogonal to the time-of-flight axis. The laser light was focused into the ionization chamber with a plano-convex quartz lens with a 200 mm focusing length. The position of the lens was adjusted to maximize the intensity of the doubly charged state of xenon. The laser energy was attenuated by a reflection-type neutral

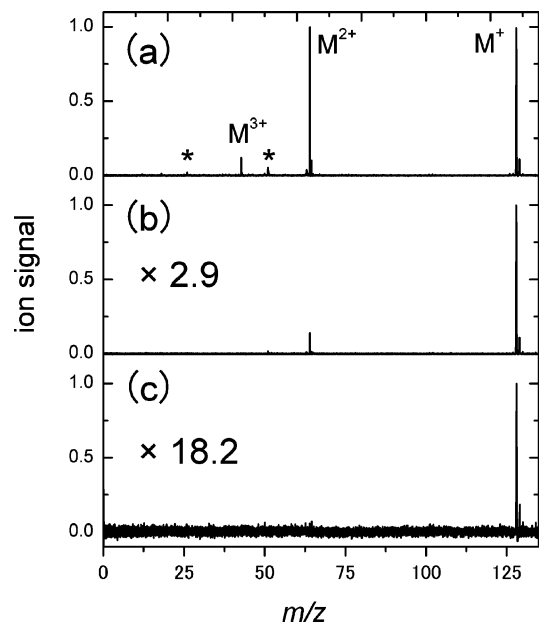


Figure 1. Mass spectra of naphthalene ionized with 1.4 μm pulses, with effective intensities of (a) 1.5×10^{14} W cm^{-2} , (b) 5.0×10^{13} W cm^{-2} , and (c) 2.1×10^{13} W cm^{-2} . M^z+ indicates the z th charged molecular ion. The original signal intensities in (b) and (c) are multiplied by 2.9 and 18.2, respectively. Asterisks in (a) indicate the fragments C_2H_2^+ ($m/z = 26$) and $(M - \text{C}_2\text{H}_2)^{2+}$ ($m/z = 51$).

density filter (Sigma Koki), and the average laser power was measured by a power meter. The actual laser intensity of the linear polarization pulse at the focus was determined by measuring the saturation intensity (I_{sat}) of xenon using the method of Hankin et al.²⁰ I_{sat} of xenon was 9.3×10^{13} W cm^{-2} (130 fs; the ADK (Ammosov–Delone–Krainov) value was multiplied by 1.12 for adjusting to the experimental value²⁰).

Results and Discussion

Ionization and Fragmentation of Naphthalene Compared with the Theoretical Calculations. Figure 1 shows the mass spectra of naphthalene ionized using 1.4 μm pulses. In contrast to the results of 0.8 μm ionization,⁸ fragmentation was strongly suppressed. The dominance of molecular ions was explained well by the nonresonance of the cation radical as in the case of anthracene:¹¹ the naphthalene cation radical does not have absorption at 1.4 μm but does have absorption at 0.8 μm .²¹ In addition, the highly charged states of naphthalene molecular ions were clearly observed up to 3+. It is also noteworthy that the distribution of fragment ions was different from that of the electron impact ionization spectrum. No ions were found in the range of $m/z = 70$ –127. This means that the lowest energy fragmentation processes (H, C_2H_2 , and C_4H_2 loss channels, appearance energy close to 16 eV²²) were negligible. The dominant fragment was $m/z = 51$, which was assigned as $(M - \text{C}_2\text{H}_2)^{2+}$. This assignment was based on the following facts: (1) The ratio of the intensity of the peak at 51 to the intensity of the corresponding ^{13}C isotope peak appearing at $m/z = 51.5$ corresponds to the natural isotope ratio. (2) The small peak at $m/z = 52$ indicated the negligible contribution of C_4H_3^+ ($m/z = 51$).

Figure 2a shows the laser-intensity dependencies of xenon ions and naphthalene molecular ions and the total number of naphthalene fragment ions obtained with a linearly polarized pulse. The theoretical ion yield curves (except for the fragments) are also shown. The ionization rate was calculated by the ADK theory.²³ In the ADK calculation, we assumed a Gaussian

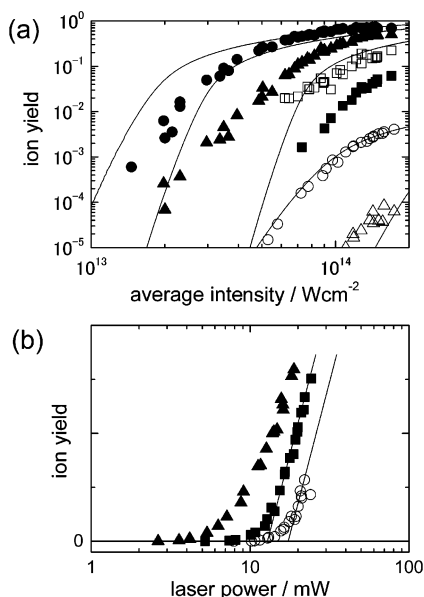


Figure 2. (a) Ion yield of naphthalene as a function of the average laser intensity of linearly polarized light: M^+ (●), M^{2+} (▲), M^{3+} (■), fragments (□). The results of Xe^+ (○) and Xe^{2+} (△) are also plotted. The ADK predictions are represented by the full curves for M^+ , M^{2+} , M^{3+} , Xe^+ , and Xe^{2+} . The average intensity is the same as the effective intensity in the case of the linearly polarized pulse. (b) Ion yield of the sum of Xe^{z+} ($z = 1, 2$) as a function of the laser power for saturation intensity (I_{sat}) determination: circularly polarized light (○), linearly polarized light (■). The ion yield of naphthalene ionized by linearly polarized light is also plotted (▲). Solid linear lines are the extrapolation from the high-intensity linear portion of the plots. The intersection with the intensity axis gives I_{sat} (saturation intensity).

(temporal and spatial) pulse and electron ejection from the p-orbital. The ion yield calculation was done under an aperture-limited²⁰ condition instead of an aperture-unlimited one.²⁴ As for naphthalene, we used 8.15 and 13.4 eV for the ionization potential of neutral and singly charged naphthalene.²⁵ The ionization potential of neutral to triply charged naphthalene has been reported previously (40 ± 5 eV), but the experimental data in this earlier study were not accurate.²⁶ We therefore estimated the ionization potential of doubly charged naphthalene as follows. The average ratio of the ionization potentials of a singly charged rare gas to those of a neutral rare gas is 2.75 ± 0.01 (average of Ar, Kr, and Xe). This value is similar to those in the cases of many organic molecules (2.64 in the case of naphthalene).²⁵ Therefore, we assumed that the average ratio of the ionization potentials of a doubly charged rare gas to those of a neutral rare gas (5.37 ± 0.02 , average of Ar, Kr, and Xe) could also be applied for the case of naphthalene. The ionization potential of doubly charged naphthalene was assumed to be 22.3 eV and was used for ADK calculation. Although the ADK prediction curve of Xe^+ fit well with the experimental data, the ADK predictions of naphthalene molecular ions deviated from the experimental data. The significant discrepancy between the experimental results and ADK predictions for naphthalene was attributed to the suppressed ionization characteristic of the molecules and also to the clear failure of the ADK prediction as the ionization potential decreased. These features are a very important topic in the study of molecular ionization and are discussed for diatomic molecules and large molecules.²⁷ The deviation of the experimental data of Xe^{2+} from those of ADK curves is understood to be clear evidence of electron-recollision-induced double ionization. However, the failure of ADK prediction for the case of naphthalene prevents us from judging

the electron recollision solely by a comparison with ADK curves.

Comparison under the Effective Intensity Scale: Electron-Recollision-Induced Double Ionization but Little Fragmentation Was Found. Recollision-induced¹⁵ double ionization is considered to contribute the formation of doubly charged states in atoms as well as in few-atom molecules below the sequential-double-ionization regime. The recollision-induced ionization mechanism is explained as follows: An electron tunnels through the potential distorted by a linearly polarized laser field, and then is driven by the field. The electron returns to the ion when the laser field reverses its direction. During the process, an electron gains large kinetic energy (ponderomotive force) from the laser fields. The collisional ionization is expected to occur if the impact energy is sufficient. The effect of recollision is usually examined by changing the laser polarization from linear to circular. This is because the orbit of a released electron will be altered by the laser electronic field and completely miss the ion in the case of circularly polarized light. In these examinations, we should take the effect of laser intensity changes into account. Suppose we use the laser power measured by a conventional power meter, the pulse width, and the area of laser focus to calculate the intensity (we call this the average intensity); in this case the intensity at the focus should not depend on the laser polarization. However, if we plot the ion yield as a function of laser power, the yield is higher by linearly polarized light than by circularly polarized light, as shown in Figure 2b. The importance of the electric field magnitude was pointed out in the ionization of diatomic molecules.²⁸ If we keep electronic field amplitudes the same, circularly polarized light results in 2-fold greater intensity than linearly polarized light. Therefore, if the electronic field amplitude severely affects the ionization, the average intensity of the circularly polarized pulse should be multiplied by 0.5 to have the same ion yield. However, the simple multiplication of average intensity fails to match the ion yield, indicating the complicated nature of ionization. To elucidate the problem, Suresh et al. introduced a scaling factor derived from the ADK calculation under the assumption that the sequential ionization rate of an atom is independent of the polarization of the external electric field.²⁹ To have the same ionization rate for both linearly and circularly polarized pulses, the average intensity is multiplied by 0.65 in the case of circularly polarized light. However, the factor that converts the average to the effective intensity was derived from theoretical calculations, and it may contain some ambiguity because the region of sequential ionization is almost flat along with the intensity. We therefore introduced another way to find the scaling factor. Assuming the sequential ionization rate is independent of laser polarization, it is also useful to use an experimental correction factor: the saturation intensity (I_{sat}) of a rare gas. I_{sat} is defined as the point at which the ion yield, extrapolated from the high-intensity linear portion of the curve, intersects the intensity axis.²⁰ This value was used to determine the actual intensity at the focus (linearly polarized pulse). The matching sequential ionization rates correspond to the shift in the I_{sat} of circularly polarized light to that of linearly polarized light. Then, from Figure 2b, we obtained a scaling factor of 0.75. The I_{sat} of naphthalene was calculated to be 5.5×10^{13} W cm⁻² by comparing the I_{sat} of Xe. The accuracy of this factor depends on how much we can obtain the linear portion of the ion yield at a higher intensity regime. Since we measured the ion yield under the same conditions (except the ellipticity), the slope, which is dependent on the concentration of neutral xenon, instrument sensitivity, and beam focusing condi-

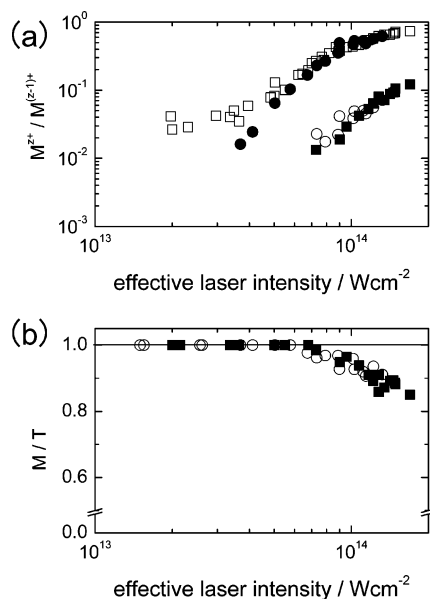


Figure 3. (a) Ratio of doubly to singly charged, $z = 2$ (●, □) and triply to doubly charged, $z = 3$ (○, ■) molecular ions plotted as a function of the effective laser intensity. Circles and squares indicate circularly polarized and linearly polarized light, respectively. (b) Ratio of the sum of molecular ions of all charge states (M) to total ions (T) including all charge states of molecular ions and fragment ions: circularly polarized light (○), linearly polarized light (■).

tion, of the linear portion is assumed to be the same. Thus, we obtained a good accuracy even though the linear portion of the data obtained by circularly polarized light was not sufficient.

Figure 3a shows the ion yield ratios among different charge states as a function of the effective instead of average laser intensity, as described above. A clear deviation of the data with linearly polarized light from those with circularly polarized light in M^{2+}/M^+ was observed below $5 \times 10^{13} \text{ W cm}^{-2}$ on the effective intensity scale. The deviation in Figure 3a provides clear evidence of electron-recollision-induced double ionization (M^{2+} formation). We observed M^{2+} at $2 \times 10^{13} \text{ W cm}^{-2}$, but the electron impact energy (11.6 eV) at this intensity was smaller than the ionization potential of M^+ (13.4 eV).²⁵ However, inelastic-scattering-induced excitation of cation radicals (the minimum energy for excitation is around 1.75 eV, as derived from the absorption spectrum of the naphthalene cation)²¹ is possible. After the excitation, tunnel ionization of the excited-state cation may occur over the next few cycles of laser pulses. In the case of rare gases, it is useful to compare the experimental data of the doubly charged ion yield with the ADK prediction, because the deviation of the experimental data from the ADK curve can be easily recognized and assigned to the electron recollision (Xe^{2+} in Figure 2a). However, the failure of ADK prediction for the case of naphthalene (Figure 2a) prevents us from judging the electron recollision solely by a comparison with the ADK curves. On the other hand, a comparison between the data obtained by linearly polarized light and those obtained by circularly polarized light under the same effective intensity scale enables us to distinguish the electron recollision very clearly (Figure 3a). Numerous studies have suggested the importance of electric field amplitude, but none have attempted to compare the ion yields obtained by linearly polarized and by circularly polarized light under the same effective intensity scale. We considered that a comparison under the same effective intensity scale would be highly useful for studying cases of

molecular ionization (especially for the molecules with low ionization potential).

In contrast to the results of double ionization, the contribution of molecular ions (M) to the total ions (T) including all charge states of molecular ions and fragment ions did not differ between linearly and circularly polarized pulses over the whole intensity regime, as shown in Figure 3b. Below $7 \times 10^{13} \text{ W cm}^{-2}$ (this value corresponds to the maximum recollision energy of 40.6 eV), there was no fragmentation. Moreover, there was no difference between the results by linearly and circularly polarized light above $7 \times 10^{13} \text{ W cm}^{-2}$. The results of doubly charged molecular ion formation clearly indicated the existence of electron recollision. However, these results strongly suggested that there was no electron-recollision-induced fragmentation even when the impact energy was sufficiently high. These differences can be understood as follows. At first, only the single-electron bombardment is expected, because the possibility of multiple collisions is small due to the Coulomb focusing and/or defocusing by the ion core.¹⁶ The low efficiency of fragmentation could be attributed to the slow fragmentation rate due to the energy distribution over all of the vibrational modes of the molecules. The dissociation occurred at a statistical rate in this case. As the molecular size increases, the number of vibrational modes increases and then the fragmentation rate decreases. The dissociation rate of naphthalene cation was evaluated by RRKM theory.²² Both hydrogen loss and acetylene loss channels exceed 10^6 s^{-1} at an internal energy of 10 eV. The acceleration time in the time-of-flight mass spectrometer is about $0.3 \mu\text{s}$ ($m/z = 128$); therefore, the fragment ion should be detected at a certain m/z if the reaction rate is higher than $3 \times 10^6 \text{ s}^{-1}$. However, a negligible number of H loss ($m/z = 127$) or acetylene loss ($m/z = 102$) fragments were observed. In addition, no fragment appeared at irregular m/z , indicating that there was no fragmentation in the field-free region. All the results indicated that the electron bombardment did not transfer sufficient energy to the naphthalene cation radicals for fragmentation. It is concluded that the efficiency of energy transfer from the electron translational energy to the vibrational energy of the molecule is low and the molecular ion received energy lower than 10 eV.

We observed $(M - \text{C}_2\text{H}_2)^{2+}$ and C_2H_2^+ as major fragment ions in the high-intensity region, indicating that the fragmentation occurred at highly charged states (perhaps in M^{3+}). The fact that the appearance intensity of the fragment ions resembled that of M^{3+} supports this hypothesis (Figure 2a). Thus, we concluded that the fragmentation originated in the unstable nature of the highly charged molecular ion itself and in the Coulomb explosion at the high-intensity region. In the case of C_{60} , up to C_{60}^{12+} was observed³⁰ and the electron-recollision-induced fragmentation was observed only at highly charged states (C_{60}^{3+} and C_{60}^{4+}).¹⁹ In contrast to the case of C_{60} (in which C_2 emission from C_{60} required more than 9.5 eV³¹), hydrocarbons were not stable at the highly charged states, because they have many C–H bonds, and the dissociation energy of the cation radical is smaller than (around 0.33–0.77 times)³² that of a neutral molecule. In addition, there exist energetically favored dissociation channels such as C_2H_2 elimination in the case of naphthalene, anthracene, and benzene. To elucidate the mechanisms of fragmentation, high intensity at a longer wavelength is necessary. We are now constructing an OPA system for producing high power and a short pulse at longer wavelengths to study ionization and Coulomb explosion.

Finally, it is worthwhile to emphasize that a significant level of fragmentation occurred under the resonant condition of the

naphthalene molecular ion (0.8 μm).⁸ In this study, we performed the ionization under a nonresonant condition (1.4 μm) for both the neutral and cationic naphthalene and found that electron recollision made only a negligible contribution to the fragmentation. We can conclude that the resonant-induced fragmentation⁷ surpasses the electron-recollision-induced fragmentation.

Acknowledgment. The present research was financially supported by a Grant-in-Aid (No. 14077214) from the Ministry of Education, Culture, Sports, Science and Technology, Japan, to N.N. We thank Mr. Hervé Jousselein of Thales Laser Co. for his kind contribution to our laser system.

References and Notes

- (1) Levis, R. J.; DeWitt, M. J. *J. Phys. Chem. A* **1999**, *103*, 6493.
- (2) Nakashima, N.; Shimizu, S.; Yatsuhashi, T.; Sakabe, S.; Izawa, Y. *J. Photochem. Photobiol., C* **2000**, *1*, 131.
- (3) Nakashima, N.; Yatsuhashi, T.; Murakami, M.; Mizoguchi, R.; Shimada, Y. In *Advances in Multiphoton Processes and Spectroscopy*; Lin, S. H.; Villaeys, A. A.; Fujimura, Y., Eds.; World Scientific Publishing: Singapore, 2005; Vol. 17.
- (4) DeWitt, M. J.; Levis, R. J. *J. Chem. Phys.* **1995**, *102*, 8670.
- (5) Ledingham, K. W. D.; Singhal, R. P.; Smith, D. J.; McCanny, T.; Graham, P.; Kilic, H. S.; Peng, W. X.; Wang, S. L.; Langley, A. J.; Taday, P. F.; Kosmidas, C. *J. Phys. Chem. A* **1998**, *102*, 3002.
- (6) Tang, X. P.; Becker, A.; Liu, W.; Sharifi, M.; Kosareva, O.; Kandidov, V. P.; Agostini, P.; Chin, S. L. *Phys. Rev. A* **2005**, *71*, 045401.
- (7) Robson, L.; Ledingham, K. W. D.; McKenna, P.; McCanny, T.; Shimizu, S.; Yang, J. M. *J. Am. Soc. Mass Spectrom.* **2005**, *16*, 82.
- (8) Harada, H.; Shimizu, S.; Yatsuhashi, T.; Sakabe, S.; Izawa, Y.; Nakashima, N. *Chem. Phys. Lett.* **2001**, *342*, 563. Harada, H.; Tanaka, M.; Murakami, M.; Shimizu, S.; Yatsuhashi, T.; Nakashima, N.; Sakabe, S.; Izawa, Y.; Tojo, S.; Majima, T. *J. Phys. Chem. A* **2003**, *107*, 6580.
- (9) Markevitch, A. N.; Romanov, D. A.; Smith, S. M.; Schlegel, H. B.; Ivanov, M. Yu.; Levis, R. J. *Phys. Rev. A* **2004**, *69*, 013401.
- (10) Robson, L.; Ledingham, K. W. D.; Tasker, A. D.; McKenna, P.; McCanny, T.; Kosmidas, C.; Jaroszynski, D. A.; Jones, D. R.; Lssac, R. C.; Jamieson, S. *Chem. Phys. Lett.* **2002**, *360*, 382.
- (11) Campbell, E. E. B.; Hansen, K.; Hoffmann, K.; Korn, G.; Tchapyguine, M.; Wittmann, M.; Hertel, I. V. *Phys. Rev. Lett.* **2000**, *84*, 2128.
- (12) Murakami, M.; Mizoguchi, R.; Shimada, Y.; Yatsuhashi, T.; Nakashima, N. *Chem. Phys. Lett.* **2005**, *403*, 238.
- (13) Trushin, S. A.; Fuss, W.; Schmid, W. E. *J. Phys. B* **2004**, *37*, 3987.
- (14) Keldysh, L. V. *Sov. Phys. JETP* **1965**, *20*, 1307.
- (15) Lezius, M.; Blanchet, V.; Rayner, D. M.; Villeneuve, D. M.; Stolow, A.; Ivanov, M. Yu. *Phys. Rev. Lett.* **2001**, *86*, 51. Lezius, M.; Blanchet, V.; Ivanov, M. Yu.; Stolow, A. *J. Chem. Phys.* **2002**, *117*, 1575. Smits, M.; de Lange, C. A.; Stolow, A.; Rayner, D. M. *Phys. Rev. Lett.* **2004**, *93*, 203402. Smits, M.; de Lange, C. A.; Stolow, A.; Rayner, D. M. *Phys. Rev. Lett.* **2004**, *93*, 213003.
- (16) Corkum, P. B. *Phys. Rev. Lett.* **1993**, *71*, 1994.
- (17) Bhardwaj, V. R.; Aseyev, S. A.; Mehendale, M.; Yudin, G. L.; Villeneuve, D. M.; Rayner, D. M.; Ivanov, M. Yu.; Corkum, P. B. *Phys. Rev. Lett.* **2001**, *86*, 3522.
- (18) Rajgara, F. A.; Krishnamurthy, M.; Mathur, D. *J. Chem. Phys.* **2003**, *119*, 12224. Rajgara, F. A.; Krishnamurthy, M.; Mathur, D. *Phys. Rev. A* **2003**, *68*, 023407. Krishnamurthy, M.; Mathur, D. *Phys. Rev. A* **2000**, *61*, 063404.
- (19) Bhardwaj, V. R.; Rayner, D. M.; Villeneuve, D. M.; Corkum, P. B. *Phys. Rev. Lett.* **2001**, *87*, 253003.
- (20) Bhardwaj, V. R.; Corkum, P. B.; Rayner, D. M. *Phys. Rev. Lett.* **2004**, *93*, 043001.
- (21) Hankin, S. M.; Villeneuve, D. M.; Corkum, P. B.; Rayner, D. M. *Phys. Rev. A* **2001**, *64*, 013405.
- (22) Shida, T. *Electronic Absorption Spectra of Radical Ions*; Elsevier: New York, 1988.
- (23) Jochims, H. W.; Rasekh, H.; Rühl, E.; Baumgärtel, H.; Leach, S. *J. Phys. Chem.* **1993**, *97*, 1312. Gotkis, Y.; Oleinikova, M.; Naor, M.; Lifshitz, C. *J. Phys. Chem.* **1993**, *97*, 12282.
- (24) Ammosov, M. V.; Delone, N. B.; Krainov, V. P. *Sov. Phys. JETP* **1986**, *64*, 1191.
- (25) Posthumus, J. H.; McCann, J. F. In *Molecules and Clusters in Intense Laser Fields*; Posthumus, J. H., Ed.; Cambridge University Press: Cambridge, U.K., 2001.
- (26) Tobita, S.; Leach, S.; Jochims, H. W.; Rühl, E.; Illenberger, E.; Baumgärtel, H. *Can. J. Phys.* **1994**, *72*, 1060.
- (27) Dorman, F. H.; Morrison, J. D. *J. Chem. Phys.* **1961**, *351*, 575.
- (28) Muth-Böhm, J.; Becker, A.; Faisal, F. H. M. *Phys. Rev. Lett.* **2000**, *85*, 2280. Muth-Böhm, J.; Becker, A.; Chin, S. L.; Faisal, F. H. M. *Chem. Phys. Lett.* **2001**, *337*, 313. Guo, C. *Phys. Rev. Lett.* **2000**, *85*, 2276.
- (29) Sakai, H.; Larsen, J. J.; Wendt-Larsen, I.; Olessen, J.; Corkum, P. B.; Stapelfeldt, H. *Phys. Rev. A* **2003**, *67*, 063404. Guo, C.; Gibson, G. N. *Phys. Rev. A* **2001**, *63*, 040701.
- (30) Suresh, M.; McKenna, J.; Srigengan, B.; Williams, I. D.; English, E. M. L.; Stebbings, S. L.; Bryan, W. A.; Newell, W. R.; Divall, E. J.; Hooker, C. J.; Langley, A. J. *Nucl. Instrum. Methods Phys. Res., Sect. B* **2005**, *235*, 216.
- (31) Bhardwaj, V. R.; Corkum, P. B.; Rayner, D. M. *Phys. Rev. Lett.* **2003**, *91*, 203004.
- (32) Lifshitz, C. *Int. J. Mass Spectrom.* **2000**, *198*, 1.
- (33) Zhang, X.-M.; Bordwell, F. G. *J. Am. Chem. Soc.* **1992**, *114*, 9787.